Minerals Engineering 211 (2024) 108695

Contents lists available at ScienceDirect

Minerals Engineering

journal homepage: www.elsevier.com/locate/mineng

Novel strategy for improved sylvite flotation through controlled crystallization

Yuan Yuan [a,b,c], Weiquan Zhan [a,b,d], Yang Tian [a,b], Alejandro López Valdivieso [c], Hao Yi [a,b], Shaoxian Song [a,b,*], Luis A. Cisternas [e], Feifei Jia [a,b,*]

[a] Key Laboratory of Green Utilization of Critical Non-metallic Mineral Resources of Ministry of Education, Wuhan, Hubei 430070, China
[b] School of Resources and Environmental Engineering, Wuhan University of Technology, Wuhan 430070, China
[c] Doctorado Institucional de Ingeniería y Ciencia de Materiales, Universidad Autonoma de San Luis Potosi, Av. Manuel Nava 6, Zona Universitaria, C.P. 78290, San Luis Potosi, Mexico
[d] Instituto de Física, Universidad Autonoma de San Luis Potosi, Av. Manuel Nava 6, Zona Universitaria, C.P. 78290, San Luis Potosi, Mexico
[e] Departamento de Ingeniería Química y Procesos de Minerales, Universidad de Antofagasta, Antofagasta, Chile

ARTICLE INFO

Keywords:
Crystallization
KCl
Flotation
Surface area
Interaction

ABSTRACT

By understanding minerals as crystals, a crystallization-controlled methodology was performed to enhance the floatability of soluble minerals. Here, aimed strategies were applied to modulate the crystallization of KCl salt to grow crystals with various shapes as cubic-, hopper- and needle-like structure. Stereoscope and scanning electronic microscopy (SEM) helped to unveil the morphologies where X ray diffraction (XRD) characterized their high crystallinities. Afterwards, Atomic Force Microscope (AFM) was performed to research the crystallizing behaviors that cubic-like structure was obtained by turbid fast growth, while hopper-like structure formation was due to the constant high supersaturation and needle-like crystal occurred under still fast crystallization. Flotation tests with octadecylamine hydrochloride (ODA) as collector demonstrated the floatability of samples obeyed the order as needle-like (96.19 %) > hopper-like (81.59 %) > cubic-like (80.08 %) KCl samples. The mechanism was studied by surface area and related interaction tests. BET result demonstrated the highest surface area of needle-like structure than that of hopper-like and cubic-like structure. Besides, induction time combined with adhesion & desorption force tests further explained the better interaction of needle-like sample with bubble than cubic-like sample. While the special structure of hopper-like structure with lower weight but inner filled solution resulted in its near equivalent floatability with cubic-like sample. In conclusion, a new strategy for promoting flotation behavior by designing the crystallization of soluble KCl was proposed, shedding some light on further application on other soluble or semi-soluble minerals.

1. Introduction

As one of the most valued treasures from our planet, minerals(Potter and Rossman, 1977) always contain high value of resources such as steel (Huijgen et al., 2005), iron(Garvie and Buseck, 1998), copper(Chandra and Gerson, 2009), *et al*(Zhan et al., 2022). Apart from those insoluble materials, there are also other soluble or semi-soluble minerals including phosphogypsum(Aminul Haque et al., 2020; Silva et al., 2022), calcium carbonate(Morse et al., 2007), fluorite(Gao et al., 2021) and another important type - inorganic salts like sylvinite(Kilic and Kilic, 2005). The froth flotation(Celik et al., 2002; Farrokhpay, 2012; Xie et al., 2021) has been wildly used as a powerful method to recover most kinds of minerals. Tons of efforts have been devoted to improve the flotation recovery by various methods including exploring new types of collectors (Peleka et al., 2018; Wu et al., 2016; Zhang et al., 2023), using different grinding medium(Farrokhpay, 2012; Peng and Grano, 2010; Zhang et al., 2021), adjusting mineral surficial properties(Ju et al., 2023; Lin et al., 2022; Tang and Tong, 2020). However, most of those methods focus on the trailing-end modulation instead of improving the mineral properties hindering the flotation process such as exposing faces, shapes and many other varieties that may bring out the better recovery of minerals themselves. To solve the flotation problem, it's vital to study the intrinsic properties of minerals so as to yield a direct control for ideal floatability.

* Corresponding authors.
E-mail addresses: ssx851215@whut.edu.cn (S. Song), feifeijia@whut.edu.cn (F. Jia).

https://doi.org/10.1016/j.mineng.2024.108695
Received 4 February 2024; Received in revised form 7 April 2024; Accepted 8 April 2024
Available online 12 April 2024

One important feature of minerals is that most of them pertained to crystals with regularly arrangement of repeating units(Li et al., 2022; Xu et al., 2018; Zhan et al., 2019). In nature, they grow under certain conditions so as to exhibit predictable shapes according to their belonging crystal types(Brooks and Andrews, 1974; Chopard et al., 1991; Ehrlich, 1996). For instance, quartz was found with columnar shapes in clusters since its composing component SiO_2 belonged to tripartite or hexaxite crystal system while diamond was more found to be isolated ones with composing C element arranged by isoaxial crystal system rules(Ihinger and Zink, 2000; Iwasaki and Iwasaki, 2002; Zhang et al., 2019). Among the broad types of natural minerals which require long period to form, soluble and semi-soluble minerals had the advantage to re-grow when contacting with liquid(Foucaud et al., 2021; Hoang et al., 2018), enlightening the idea of controllable design during crystallization process.

Sylvite(Filippov et al., 2021; Monte and Oliveira, 2004; Thy et al., 2006), as the main resource of potassium element, has been stressing researchers' attention as fertilizer, medicine and aerospace materials. Meanwhile, sylvite is also a kind of mineral constituent by KCl crystal with cubic crystal system and high solubility in water(Osipova et al., 2022; Weedon et al., 2007). Moreover, its solubility highly relies on solution temperature which promises the possibility to improve the flotation recovery by designing the crystallization process in solution(Li et al., 2015). As mentioned above, the soluble and semi-soluble minerals share the advantage to be re-constructed according to the later requirements(Ejtemaei et al., 2014; Feng et al., 2022; Marion et al., 2020) like lower dosage of collector and foaming reagent, stronger interaction force with bubbles, greater difference with tailings, *et, al*, in order to yield a better flotation recovery.

Here, taking sylvite as an example, crystal growth of its composing crystal KCl was well designed to produce samples with different shapes and their related flotation behaviors were also described. By modulating the crystallization of KCl through solution temperature combined with evaporation and system turbulence, various shapes including cubic-, hopper- and needle-like KCl crystals were obtained without additional reagents. Afterwards, their different crystallization behavior was revealed by AFM. Flotation tests and related mechanisms were further researched in detail. This work paved a path to promote the flotation by modulating the crystallization process for soluble and semi-soluble minerals.

2. Materials and methods

2.1. Materials

Analytical pure grade KCl reagent (Sinopharm Chemical Reagent Co., Ltd., China) and deionized water (Millipore SAS, France) with resistivity as 18.2 MΩ·cm were mixed to prepare the saturated KCl solution to eliminate undesirable ions. ODA with analytical requirement of purity was purchased from Aladdin Pharmacy company, China.

2.2. Preparation of KCl crystals with various shapes

The key idea of modulating the KCl crystal structure is to adjust the oversaturation to control the growth preference. Solubility of KCl highly depends on the temperature. For KCl crystallization process, the interface area of gas–liquid, turbulence of solution system as well as cooling conditions greatly affect the supersaturation thus further influent the growth of KCl crystals. Hence, various strategies have been tried to prepare cubic-like, needle-like and hopper-like KCl crystals and the detailed methods are described as below. Notably, all samples were totally dried and then divided into different size ranges by standard dry sieving technique. Samples with size between 180 and 250 μm were prepared for later flotation in order to exclude the influence of particle size factor.

2.2.1. Preparation of cubic-like KCl crystals

It's known the fact that crystal habit of KCl is cubic structure. Here, a relatively fast but uniform crystallization method was performed to collect cubic samples. First, 100 mL saturate solution of 55 °C was prepared and heated up to 60 °C with a foil covered tightly to avoid evaporation of water. The transparent solution was then transferred to cold water bath at 0 °C using ice-water mixture with stirring speed as 400 rpm for 2 h. Afterwards, the grown cubic crystals with wide size distribution were filtered and dried up in an oven at 45 °C for overnight.

2.2.2. Preparation of hopper-like KCl crystals

The formation of hopper-like KCl crystals appeared under constant high value of oversaturation during crystallization of HCC crystals, which had been reported in previous work(Desarnaud et al., 2018). Similarly, a cooling process assisted by a constant speed programmable thermostatic bath machine (XOYS-2010 N, ATPIO Lcd., Nanjing, China). A designed vertical cylindrical jacketed crystallizer with 250 mL capacity was connected to the warm bath to realize a constant cooling process from 30 °C to 27 °C with 3 °C/h cooling rate. During this period, the corners of one cubic structure got the chance to grow faster to form hopper-like structure with large exposing (2 0 0) face area and relatively hollow cubic shape. These hopper-like KCl crystals were obtained in order to compare the flotation behavior with needle-like and cubic-like KCl crystals.

2.2.3. Preparation of needle-like KCl crystals

The needle-like formation of KCl crystals was due to the faster growth of KCl under one-dimension shape with a high level of supersaturation which means two ways including high cooling rate and evaporating rate. In order to yield the needle-like crystals, a combined method of cooling and evaporating was performed here. Similar to method of cubic-like sample, saturate KCl solution at 70 °C was prepared by adding weighed reagent to a proper amount of DI water and heat to 75 °C with a foil cover. Afterwards, the clear solution was immediately transferred to ice bath to accelerate the crystallization process but kept still. Notably, the cover was removed to let evaporation occur at the same time with cooling process. At the primary step, several thin and small needle-like crystals appeared on the surface of solution, *i.e.*, the liquid–gas interface, where the higher concentration of K and Cl ions under fast water evaporation condition helped needles to grew longer and thicker. During this period, due to the gravity, most of them fell down to the bottom of solution where they could further grow while maintaining the initial shape of needle structure.

2.3. Experimental design

2.3.1. Micro-flotation experiments

Batch flotation experiments were performed with a flotation machine equipped with 60 mL cell. Typically, 15 g samples were added into 60 mL saturated KCl solution and conditioned for 5 min. Subsequently, the mixture was poured into the cell and ODA was added as collector. It's worth mentioning that the flotation of KCl occurs only when concentration of ODA exceeds its solubility to work in form of flocs(Du et al., 2014). A proper concentration as 5.56×10^{-5} mol/L of ODA(Li et al., 2016; Zhou et al., 2021) was chosen to value the floatability of KCl samples. Samples were floated for 2 min with air at a flow rate of 50 cm^3/min. All flotation tests were conducted under room temperature as ~ 25 °C.

2.3.2. Induction time tests

The set up was a self-made system with a platform for controllable movement of the tip with bubble. By connecting an industrial camera, the reacting moment of bubble with sample particles could be recorded. For each condition, the approaching and retracting process as one movement were repeated for 20 times to calculate the adhesion probability. With increasing reacting period, tests of various adhesion probability were obtained ant the period with 50 % adhesion probability was thought to be induction time.

2.3.3. Adhesion & adsorption force tests

The interaction between aiming minerals with bubbles and collectors also relies on their adhesion as well as adsorption force. Here, the related force tests of needle-, hopper- and cubic- like KCl crystals and saturated KCl solution were determined by a surface tension meter (Powereach JK99M2, China). Firstly, KCl samples with various structure and 180–250 μm were immersed in saturated KCl solution involving 5.56 × 10^{-5} mol/L ODA collector for 6 min in order to show the interaction force during real flotation process. Afterwards, the filtered and dried samples were carefully settled on the bottom of a container to make a flat mineral bed for later tests. The droplet of 100 μL KCl was attached to a needle with a small ring with diameter around 1 mm as tip, where the other end was connected to a micro force sensor with high sensibility as ~ 0.1 μN. During a typical adhesion & adsorption force test, the saturated KCl with a flat mineral bed composed by KCl particles on the bottom was put on the lifting platform with 2 mm distance from the bottom of KCl droplet. Notably, the gravity of droplet was cleared to zero before each test to get a better curve with baseline recoupling with x axis which helped reading interacted forces. The real time changes of reacted force on the droplet were recorded by the micro force sensor and adhesion & adsorption force data could be obtained with the data analyze.

2.3.4. AFM tests

The morphologies of various micro needle-like KCl crystal and surface of cubic-like KCl crystals were tested by AFM (Bruker MM8, Germany). For needle-like sample, to study the mechanism of needle structure formation, a spinner was used to get a high speed of KCl solution evaporation, along with the fast growth of KCl crystals in nanometer size. Low and high concentration with 50 mg/L of KCl solutions were prepared to study the initial stage during fast growth of KCl crystals, respectively. To prepare the AFM sample, a fresh cleaved mica with 10 × 10 mm size, as the base for observation due to its layered property, was fixed on center of the spinner. Then, 10 μL of solution was dropped on surface of clean mica and spined for 300 s to ensure a good dispersion as well as fast evaporation. The mica with dispersed samples was then dried at room temperature for 12 h for morphology scanning tests by AFM. For surface of cubic KCl structure study, a mild evaporation method helped to obtain perfect cubic crystals. Here, 200 mL saturated KCl solution at 25 °C was poured into a glass made petri dish with diameter of 15 cm for more than 7 days. During the crystallization period, well-structured cubic samples were carefully picked out and dried by filter paper on the bottom to protect the flat surface. For AFM tests, the ScanAsyst Air mode in the presence of equipped with probe with silicon tip on nitride lever was used to get the surficial details and professional software NanoScope Analysis 1.4 was performed to analyze the results.

2.4. Characterization

XRD was conducted to reveal the crystallinity of crystal samples. The morphologies of grown KCl crystal with different shapes were studied by stereoscope as well as Scanning electronic microscope SEM. Fourier transform infrared spectroscopy (FTIR) was used to learn the adsorption of collector ODA with KCl samples and XPS (X-ray photoelectron spectroscopy) tests helped to understand the binding energy changes of composing elements. Size information of ODA flocs was obtained by zeta potential apparatus (Malvern Zeta-sizer Nano ZS90, UK) with suspension of ODA flocs in saturated KCl solution. The exposing surface area information was studied by the Brunauer-Emmett-Teller (BET, V-Sorb 4800P, China) in pure N_2 atmosphere.

3. Results and discussion

3.1. Crystal structure and morphology

3.1.1. Crystal structure

According to the various strategies, three types of KCl crystals were collected and their corresponding structure was studied by XRD while their morphology information was researched by stereoscope as well as SEM. As FCC crystals, the crystallinity of KCl is a key parameter of its properties. Shown in Fig. 1. were the XRD spectra of cubic-, hopper-like and needle-like structured KCl crystals. Shared narrow and sharp peaks at around 28.43, 40.60, 50.27, 58.72, 66.45 and 73.76 degrees were in coincidence with the JCPD data of KCl(Ji et al., 2022; Li et al., 2021), indicating their high purity and well crystallinity. By comparing the peaks among three samples, all possessed the strong intensity of (200) facet. The highest (200) peak of hopper-like sample and lowest of needle-like sample could be ascribed to their special structure which should be further demonstrated by the morphological result.

3.1.2. Morphology

During flotation, the shape of minerals particles always stresses great attention of all researchers. Here, the morphology of three types of KCl samples were obtained by both stereoscope on the left and SEM on the right as shown in Fig. 2. Intuitively, three samples exhibited various shapes with cubic-, hopper- and needle-like structure, respectively. It's worth noting that these crystals with different size distribution were due to the easily formation of KCl structure. Standard sieves were conducted to eliminate the size parameter before flotation tests. For first sample in Fig. 2a and 2b, particles shared even size distribution with near cubic forms that the slightly abraded corners could be ascribed to the stirring impact. Their cubic-like formation was in good agreement with its intrinsic property that KCl crystal belongs to cubic crystal system. In Fig. 2c and 2d, with constant cooling method, the higher concentration of K and Cl ions on corners lead to their preferential growth, resulting in the hopper-like structure. It's worth mentioning that hopper-like samples had a wild size distribution that one large particle was chosen in SEM test to display a detailed observation. Moreover, the needle-like structure in Fig. 2e and 2f was thought to be originated by the fast crystallization along the one-dimensional direction.

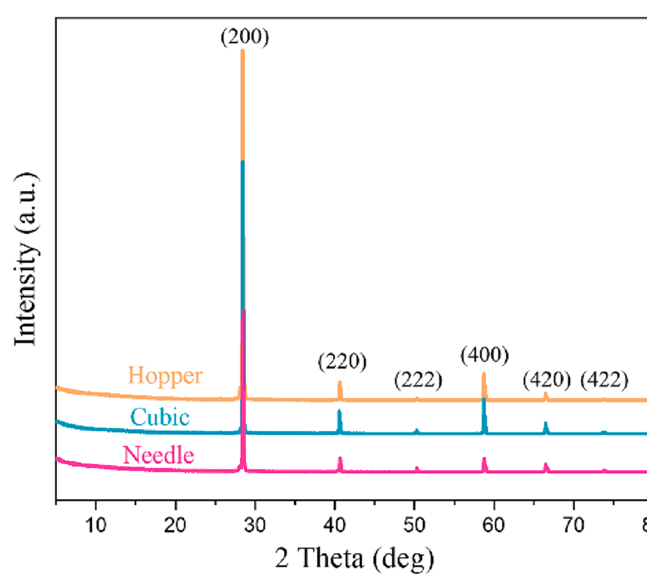

Fig. 1. XRD patterns of cubic-, hopper- and needle-like KCl crystals.

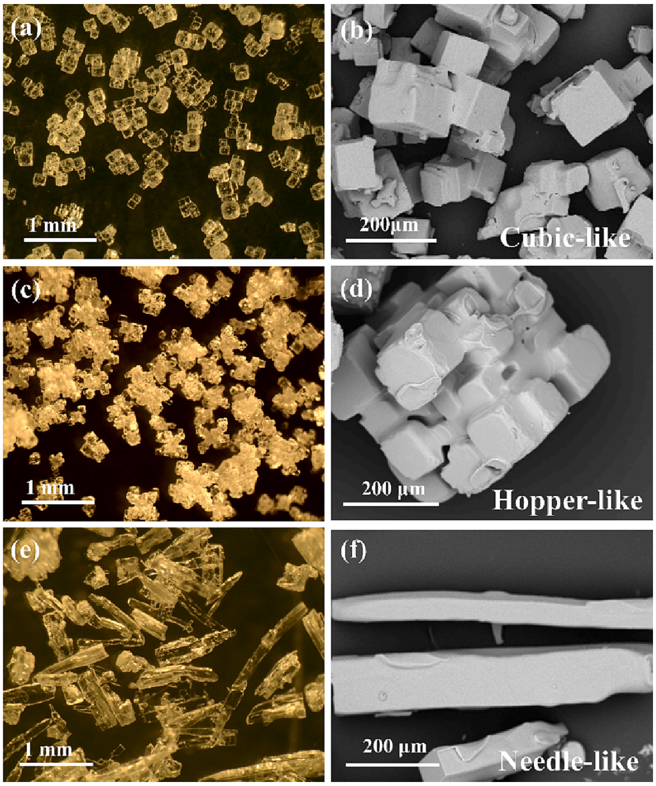

Fig. 2. Stereoscopic (left) and SEM (right) images of (a, b) cubic-, (c, d) hopper- and (e, f) needle-like KCl crystals.

3.2. Crystal growth mechanism

The successful preparation of cubic-, hopper- and needle-like crystals were precisely designed by crystallization property of KCl. However, the detailed growth behavior remains unclear which might help to understand the inner mechanism so as to pave a path to later improvement of applications. Considering that KCl belongs to FCC type crystal whose surface is supposed to be flat square, AFM could be applied to image the topography of cubic KCl structure. What's more, the needle-like crystal formation was ascribed to the fast crystallization which could be similar with the fast spin-evaporation process during preparation of AFM samples. Thus, AFM was applied to study the surface detail in microscopic level for three types of KCl crystals: mild evaporation growth for large scale cubic-like KCl, fast spin evaporated growth of 10 μL saturated solution on mica for needle-like KCl, and still evaporation of 10 μL saturated solution on mica for hopper-like KCl.

Shown in Fig. 3 are their two-dimensional AFM result with the height information of lined area inserted, and corresponding three-dimensional result. Especially, due to the relatively large scale of cubic- and hopper-KCl crystal, the morphologies of chosen crystal for surficial test was obtained by optical microscope of AFM setup as displayed in Fig. S1. The cubic crystal in Fig. S1a showed a flat square surface, providing the excellent chance for scanning its surface in nanometer scale as shown in Fig. 3a and 3b where the crystal grew by layers with height of ~ 1.0 nm which could be height of single layer of K-Cl. The seemed flat surface of cubic structure was actually full of stages as in the 3D result with abundant exposing edges.

Actually, the layered structure would be magnified by the fast still crystallization in form of arena-like structure like in Fig. S1b. Instead of the smooth formation of cubic structure during mild evaporation, the layers parallel to four edges of the upper square appeared with fast growth. The corresponding AFM results in Fig. 3c and 3d exhibited the stages-formation with height around 99.9 nm, much larger than that of cubic stage. With further growth of the arena-like structure in uniform solution environment with stirring and cooling, the stages would be amplified thus reach a well-grown branches on eight corners, showing a hopper-like structure.

In the case of needle-like structure, the relatively small size of structure hindered the observation by microscope but its 2D and 3D AFM results in Fig. 3e and 3f still helped to understand its growth details. Obviously, with the fast spin-evaporation method, the saturated KCl crystallized rapidly in form of thin and long structure, similar to needles samples during the cooling-evaporation combined strategy. The height of needle structure was about 40.3 nm which was ~ 40 folds of one single layer's height, indicating its property as KCl crystal. Although the fact that needle-like KCl possesses tiny size for microscope, it was feasible to observe its initial formation as crystal seeds during spin-evaporation process under low concentration of KCl. Here, KCl pure solution with concentration as 50 mg/L was prepared to study how the KCl would grow on surface of mica. The AFM result in Fig. S2 demonstrated that at the beginning stage of crystallization, K and Cl ions would gather together for later growth. Interestingly, with spin-evaporation during sample preparation, these ions tended to form tiny thin chains with height around 12.0 nm, in coincidence with the needle-like structure with saturated KCl solution. The mechanism of needle-like KCl crystal was concluded that with rapid crystallization, K and Cl ions firstly immigrated to form chains and then resulted in needle-like crystals.

3.3. Flotation test

With the unveiled mechanism of cubic-, hopper- and needle-like KCl crystal formation, their flotation behaviors were researched using ODA as collector, as shown in Fig. 4. The floatability was in decreasing order of needle-like > hopper-like > cubic-like, where all fit well with classical first-order model as displayed in Table 1. The highest flotation rate and recovery of needle-like KCl indicated its better interaction with ODA. Apart from needle-like structure, hopper-like structure pertained similar flotation recovery with cubic-like KCl but greater floating rate as 3.15 min^{-1} than 2.49 min^{-1}. It's reasonable to speculate that due to the special structure, hopper-like crystal with proper size could be quickly absorbed to bubbles with the four "feet" on top of branches, resulting in fast flotation rate at beginning. However, the final recovery was similar with cubic-structure indicated its limited improvement, which could be ascribed to its requirement of proper size of bubbles to be captured. For needle-like structure, its excellent flotation rate and recovery demonstrated the successful strategy of enhanced floatability of soluble crystal by manipulating its crystallization. The related mechanisms were studied as following parts.

3.4. Flotation mechanism

The good floatability of prepared cubic-, hopper- and needle-like KCl crystals suggested the possible interaction among particles, bubbles and collector ODA. To unveil flotation mechanism as well as the different behaviors of various samples, FTIR, XPS, BET, induction time and adsorption & desorption force tests were conducted as displayed as following content.

3.4.1. FTIR test

The adsorption of collector ODA on KCl crystals was first studied by FTIR. Shown in Fig. 5 were the spectra of cubic-, hopper- and needle-like KCl crystals before (grey) and after (colored) interacted with ODA during flotation process. By comparing the grey and colored curves, it was clear the three samples all exhibited new peaks at around 2917.70 and 2850.5 cm^{-1} that could be ascribed to the antisymmetric stretching vibration of methyl group (–CH_3) and the symmetric stretching strong absorption peak of methylene group (–CH_2) of ODA(Chun, 2009; Nawaz et al., 2012), demonstrating its successful adsorption on KCl crystals as collectors. The interaction type was then researched by XPS.

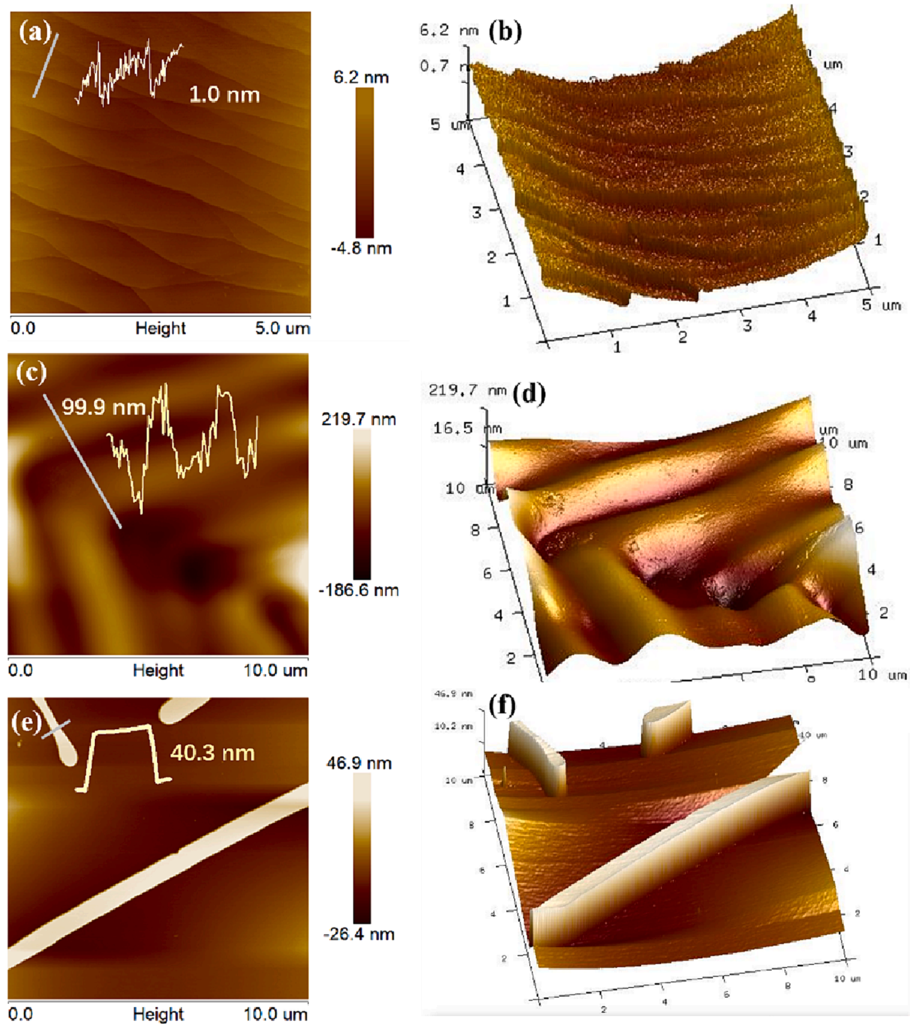

Fig. 3. Two-dimensional (left) and three-dimensional (right) AFM images of (a, b) cubic-, (c, d) hopper- and (e, f) needle-like KCl crystals.

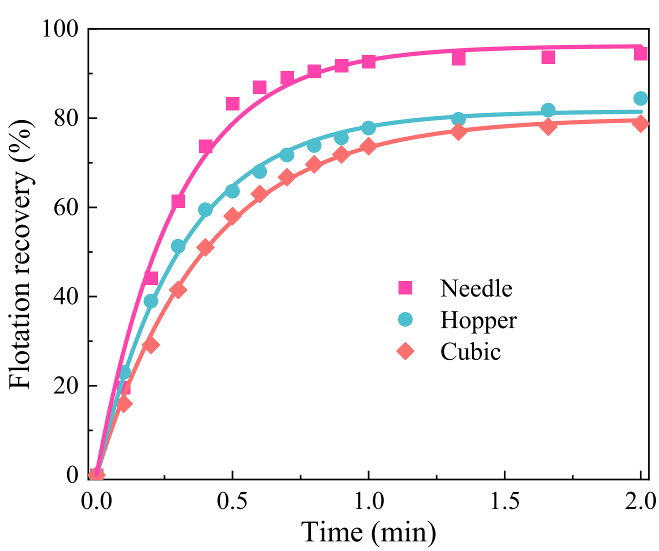

Fig. 4. Flotation kinetics results of cubic-, hopper- and needle-like KCl crystals using ODA as collector.

Table 1
Kinetic parameters for flotation kinetics of classical first-order model.

Samples	Classical first-order model		
	ε_∞(%)	k_1 (min^{-1})	R^2
Cubic-like	80.08	2.49	0.998
Hopper-like	81.59	3.15	0.997
Needle-like	96.19	3.41	0.989

3.4.2. *XPS test*

With the adsorption of ODA on KCl crystals, particles were successfully floated. The interaction between them was studied by XPS examine any new bonds where the binding energy information of K and Cl as shown in Fig. S3 and S4. The related data was listed in Table 2 to facilitate comparation the binding energy of cubic-, hopper- and needle-like KCl before and after flotation. It's clear that three of samples showed similar binding energy of K and Cl peaks before flotation, indicating the high purity of KCl component. Besides, in each case of the cubic-, hopper- and needle-like KCl crystal, there was no changes before and after the flotation process, demonstrating that there was no new chemical production after interacting with ODA. Hence, the mechanism could be ascribed to the physical interaction like static force, as reported by previous research (Cao et al., 2010).

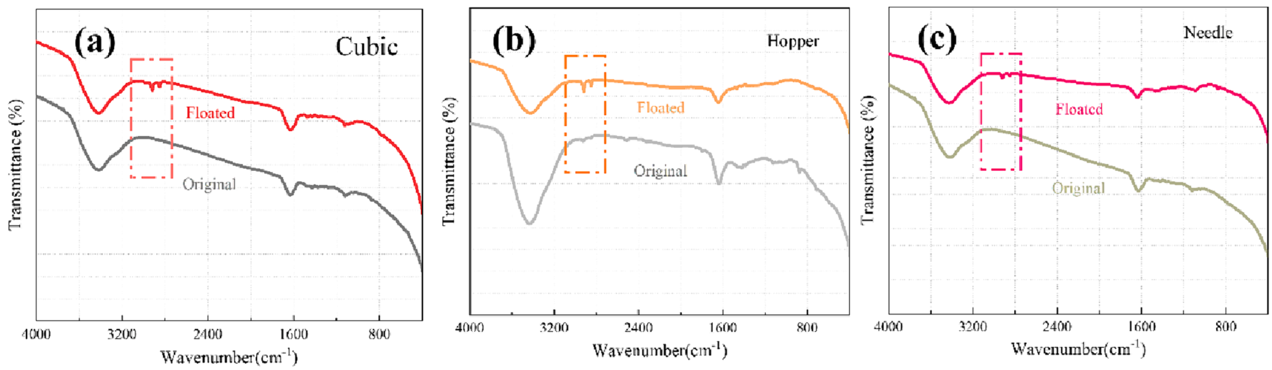

Fig. 5. FTIR results of cubic-, hopper- and needle-like KCl crystals before and after flotation with ODA as collector, respectively.

Table 2
Peaks of potassium and chloride XPS survey of cubic-, needle-, and hopper-like KCl crystals before and after flotation.

	Cubic-KCl			Needle-KCl			Hopper-KCl		
	Original (eV)	Floated (eV)	Shift (eV)	Original (eV)	Floated (eV)	Shift (eV)	Original (eV)	Floated (eV)	Shift (eV)
K	292.80	292.87	−0.07	292.65	292.84	−0.19	292.95	292.74	0.21
	295.58	295.67	−0.09	295.40	295.60	−0.20	295.72	295.50	0.22
	294.24	294.36	−0.12	293.90	294.35	−0.45	294.30	294.30	0.00
	297.02	297.20	−0.18	297.50	297.10	0.40	297.40	297.00	0.40
Cl	198.20	198.23	−0.03	197.99	198.24	−0.25	198.33	198.09	0.24
	199.85	199.83	0.02	199.53	199.81	−0.28	199.96	199.72	0.24
	200.96	200.85	0.11	200.92	200.48	0.44	201.30	201.20	0.10
	196.60	196.33	0.27	196.70	196.50	0.20	196.70	196.70	0.00

3.4.3. *BET test*

The above XRD, FTIR and XPS results suggested that the prepared cubic-, hopper- and needle-like KCl samples possessed high purity, same exposing faces while stereoscope and SEM results exhibited their various shapes as well as surface area. Here, BET tests were applied to study the surface area of KCl crystals with three shapes. Fig. 6. displayed the BET value of prepared crystals with size between 178 and 250 μm in N_2 atmosphere. The decreasing surface area values were in order of needle-like > hopper-like > cubic-like KCl crystal, in coincidence with their flotation recovery with ODA as collector. It's worth noting that different from normal collectors working as molecules, ODA in saturated salt solution with concentration higher than its CMC (4×10^{-5} mol/L) would function with flocs form. The size of those flocs relied on the concentration. In this case, the size of ODA flocs with concentration 5.56×10^{-5} mol/L in saturated KCl solution was tested by zeta potential apparatus. The tested size of flocs as ∼ 3.2 μm, similar to previous research as 2.1 μm(Fangqin, 2012), much smaller than the interstices of hopper-like structure, implying that the higher surface area of KCl crystal, the more ODA flocs would be adsorbed. As a consequence, with same weight of crystals in flotation as 15 g, the needle-like structure with higher BET value could adsorb more ODA flocs so as to yield the best flotation recovery. One other important fact was that due to the fast grow of needle-like KCl, more cracks or defects could appear on surfaces of structure which resulted in its higher BET as well as higher flotation recovery.

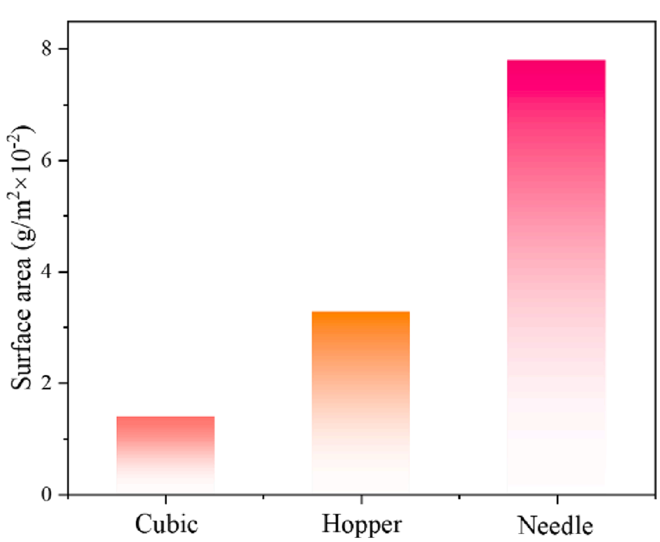

Fig. 6. BET results of cubic-, hopper- and needle-like KCl crystals with size of 178–250 μm.

3.4.4. *Induction time tests*

Apart from the adsorption amount of ODA collector, induction time was one powerful test to predict the floatability of minerals. In this work, to study the flotation behavior of cubic-, hopper- and needle-like KCl crystals, conditions of induction time tests including ODA dosage and particle size range were with kept the same with flotation process. Shown in Fig. 7. were the induction time results of three samples where needle-like KCl sample had the shortest induction time as 30 ms. While Hopper-like structure showed a longer result as 100 ms, followed by the longest induction time of cubic-like KCl as 150 ms. The consequence in an increased induction time as needle-, hopper- and cubic-like structure was in consistent with their worse flotation recovery, indicating the better interaction between needle-like structure with bubble during flotation process. Besides, the inserted three pictures of KCl samples absorbing on bubble displayed their three-phase-contact (TPC) information that needle-like structure possessed long TPC on regard of its relatively lower gravity weight. In case of hopper- and cubic-like KCl, they had similar size but similar TPC result where the former had slightly less weight due to its special structure. Notably, the four parallel faces on one side of hopper structure could be anchored on bubbles with specific size to yield a more stable interaction than the one flat square face of cubic structure. As a consequence, needle-, hopper- and cubic-

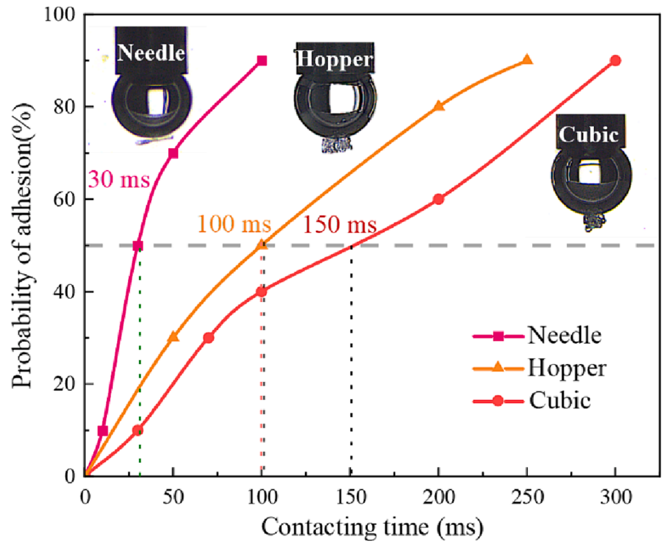

Fig. 7. Induction time results of cubic-, hopper- and needle-like KCl crystals using ODA as collector.

like structure KCl crystals showed a prolonged induction time thus behaved a declined floatability.

3.4.5. Interaction

Although induction time reveals the reaction process between mineral and bubbles during flotation, the interaction details remain unclear. Here, the adhesion and desorption forces between ODA adsorbed cubic-, hopper- and needle-like KCl crystals and saturated KCl solution were tested as displayed in Fig. 8. Grey lines showed the approaching process of the KCl saturated drop to the mineral bed where three samples all appeared a slightly jump-into force, which was read as the adhesion force value as shown in Fig. 8d. After approaching, sample bed and the drop contacted and moved together for a short time then started the retracting process with force recorded by colored lines. The desorption forces were read by the largest value where all results were exhibited in Fig. 8d. Compared with cubic-like KCl, needle-like had the lower interaction force with saturated KCl solution which implied its stronger interaction with bubble, in coincidence with the different flotation of these two samples. Nevertheless, hopper-like structure had the highest adhesion & desorption with KCl saturated solution, which could be explained by its special structure that when approaching the drop, a certain part of solution emerged in the hollow part of hopper-structure and remained there, changing its original property so as to obtain a promoted interaction force. To some extent, this disadvantage of

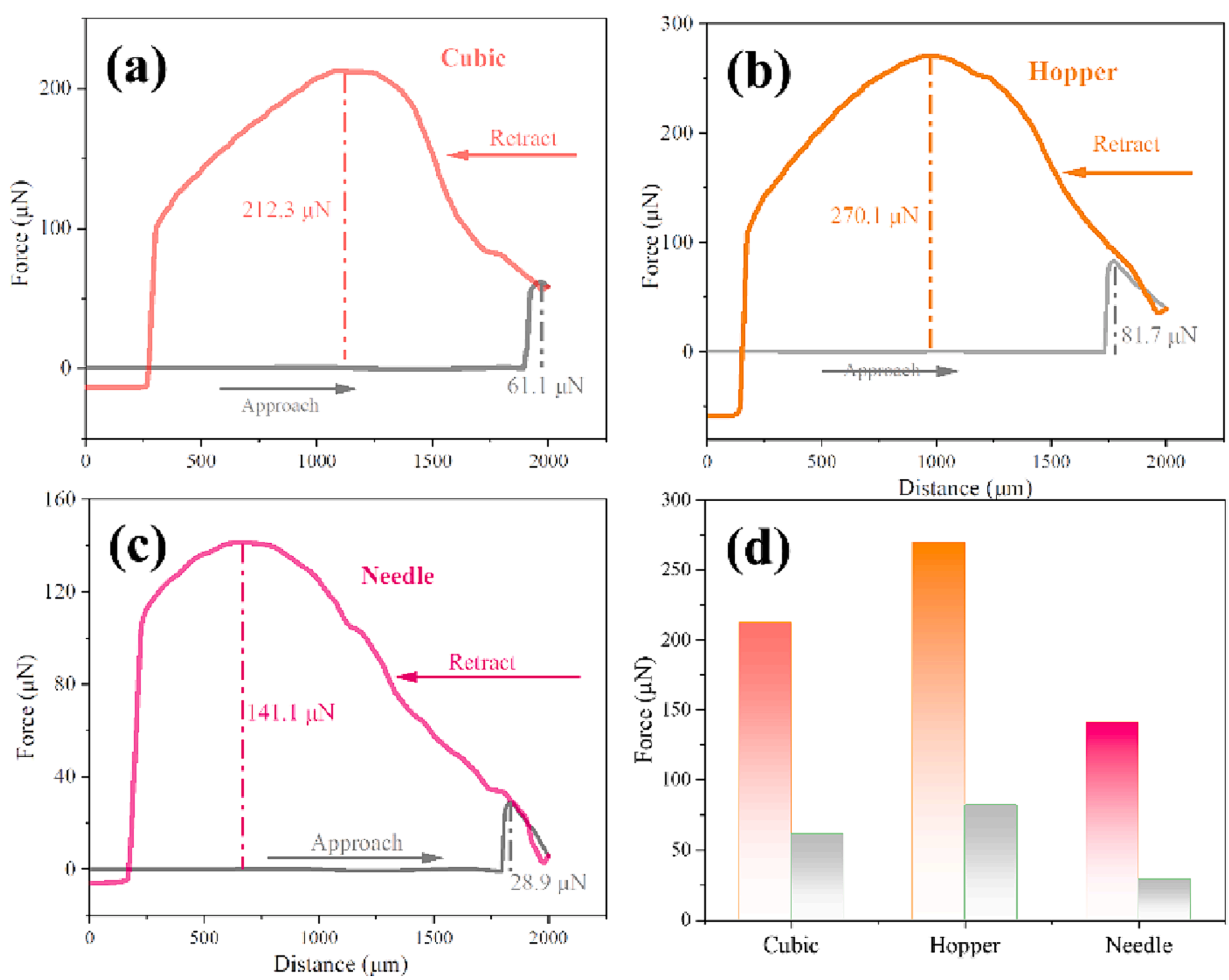

Fig. 8. Adhesion & adsorption force results of (a) cubic- (b) hopper- and (c) needle-like KCl crystals with saturated KCl drop, and (d) corresponding force information.

hopper-like structure hindered its floatability, resulting its near-equal recovery with cubic-like structure. As a result, the adhesion & desorption force tests well demonstrated the better flotation behavior of needle-like sample than cubic-like structure. Meanwhile, the special hopper-like structure had shorter induction time but a worst interaction with bubbles, exhibiting a similar flotation recovery with cubic-like samples.

4. Conclusions

In this work, a crystallization-controlled methodology was for the first time applied to enhance the flotation behavior of soluble mineral - KCl salt. Various strategies were precisely designed including fast crystallization with stirring, constant speed crystallization and fast still crystallization to grow KCl crystals with cubic-, hopper- and needle-like structure, respectively. Stereoscopy and SEM results showed their regular shape and XRD tested demonstrated their high crystallinity. The surficial information was obtained by AFM which also explained the growth mechanism. Then, the flotation tests by using ODA as collector indicated a declined recovery as needle-, hopper- and cubic-like sample, demonstrating the better performance of needle-like sample by modulating the crystallization. BET tests revealed the higher surface area of needle-like structure which could absorb more ODA flocs during flotation thus achieving a better recovery. Induction time as well as adhesion & desorption force tests further explained the faster and stronger interaction of needle-like sample with bubbles, resulting its best floatability. As a consequence, the enhanced flotation recovery of sylvite was achieved by modulation of its crystallization process, providing the methodology for other soluble minerals like hailite, picromerite and semi-soluble minerals like fluorite and phosphogypsum.

CRediT authorship contribution statement

Yuan Yuan: Writing – original draft, Methodology, Data curation, Conceptualization. **Weiquan Zhan:** Supervision, Investigation, Formal analysis. **Yang Tian:** Methodology, Investigation. **Alejandro López Valdivieso:** Supervision, Formal analysis. **Hao Yi:** Project administration, Funding acquisition. **Shaoxian Song:** Writing – review & editing, Supervision, Project administration, Funding acquisition. **Luis A. Cisternas:** Validation, Software. **Feifei Jia:** Writing – review & editing, Supervision.

Declaration of competing interest

The authors declare that they have no known competing financial interests or personal relationships that could have appeared to influence the work reported in this paper.

Data availability

Data will be made available on request.

Acknowledgements

The work is financially supported by the National Key Research and Development Program of China (2022YFC2904004). This work was partially done by Luis A. Cisternas into visit at the Wuhan University of Technology, supported by MINEDUC-UA project, code ANT 22991. Yuan gratefully acknowledges the Consejo Nacional de Humanidades Ciencias y Tecnologías (CONAHCYT) of Mexico for offering her the scholarship under the grant No. 812586 during her Ph.D. studies.

Appendix A. Supplementary data

Supplementary data to this article can be found online at https://doi.org/10.1016/j.mineng.2024.108695.

References

Aminul Haque, M., Chen, B., Liu, Y., Farasat Ali Shah, S., Ahmad, M.R., 2020. Improvement of physico-mechanical and microstructural properties of magnesium phosphate cement composites comprising with Phosphogypsum. J Clean Prod 261, 121268. https://doi.org/10.1016/J.JCLEPRO.2020.121268.

Brooks, D.B., Andrews, P.W., 1974. Mineral Resources, Economic Growth, and World Population. Science 1979 (185), 13–19. https://doi.org/10.1126/SCIENCE.185.4145.13.

Cao, Q., Du, H., Miller, J.D., Wang, X., Cheng, F., 2010. Surface chemistry features in the flotation of KCl. Miner Eng 23, 365–373. https://doi.org/10.1016/J.MINENG.2009.11.010.

Celik, M.S., Hancer, M., Miller, J.D., 2002. Flotation Chemistry of Boron Minerals. J Colloid Interface Sci 256, 121–131. https://doi.org/10.1006/JCIS.2001.8138.

Chandra, A.P., Gerson, A.R., 2009. A review of the fundamental studies of the copper activation mechanisms for selective flotation of the sulfide minerals, sphalerite and pyrite. Adv Colloid Interface Sci 145, 97–110. https://doi.org/10.1016/J.CIS.2008.09.001.

Chopard, B., Herrmann, H.J., Vicsek, T., 1991. Structure and growth mechanism of mineral dendrites. Nature 353, 409–412. https://doi.org/10.1038/353409a0.

Chun, M., 2009. Study of monolayer films formed on the subphase containing small molecule salts. Chemical Research and Application.

Desarnaud, J., Derluyn, H., Carmeliet, J., Bonn, D., Shahidzadeh, N., 2018. Hopper Growth of Salt Crystals. J. Phys. Chem. Lett. 9, 2961–2966. https://doi.org/10.1021/ACS.JPCLETT.8B01082.

Du, H., Ozdemir, O., Wang, X., Cheng, F., Celik, M.S., Miller, J.D., 2014. Flotation chemistry of soluble salt minerals: From ion hydration to colloid adsorption. Miner. Metall. Process 31, 1–20. https://doi.org/10.1007/BF03402344/METRICS.

Ehrlich, H.L., 1996. How microbes influence mineral growth and dissolution. Chem Geol 132, 5–9. https://doi.org/10.1016/S0009-2541(96)00035-6.

Ejtemaei, M., Gharabaghi, M., Irannajad, M., 2014. A review of zinc oxide mineral beneficiation using flotation method. Adv Colloid Interface Sci 206, 68–78. https://doi.org/10.1016/J.CIS.2013.02.003.

Fangqin, C., 2012. Study on Octadecylamine-HCl's Colloid Chemistry in KCl Flotation. Journal of Shanxi University.

Farrokhpay, S., 2012. The importance of rheology in mineral flotation: A review. Miner Eng 36–38, 272–278. https://doi.org/10.1016/J.MINENG.2012.05.009.

Feng, Q., Yang, W., Wen, S., Wang, H., Zhao, W., Han, G., 2022. Flotation of copper oxide minerals: A review. Int J Min Sci Technol 32, 1351–1364. https://doi.org/10.1016/J.IJMST.2022.09.011.

Filippov, L.O., Filippova, I.V., Barres, O., Lyubimova, T.P., Fattalov, O.O., 2021. Intensification of the flotation separation of potash ore using ultrasound treatment. Miner Eng 171, 107092. https://doi.org/10.1016/J.MINENG.2021.107092.

Foucaud, Y., Lainé, J., Filippov, L.O., Barrès, O., Kim, W.J., Filippova, I.V., Pastore, M., Lebègue, S., Badawi, M., 2021. Adsorption mechanisms of fatty acids on fluorite unraveled by infrared spectroscopy and first-principles calculations. J Colloid Interface Sci 583, 692–703. https://doi.org/10.1016/J.JCIS.2020.09.062.

Gao, Z., Wang, C., Sun, W., Gao, Y., Kowalczuk, P.B., 2021. Froth flotation of fluorite: A review. Adv Colloid Interface Sci 290, 102382. https://doi.org/10.1016/j.cis.2021.102382.

Garvie, L.A.J., Buseck, P.R., 1998. Ratios of ferrous to ferric iron from nanometre-sized areas in minerals. Nature 396, 667–670. https://doi.org/10.1038/25334.

Hoang, D.H., Kupka, N., Peuker, U.A., Rudolph, M., 2018. Flotation study of fine grained carbonaceous sedimentary apatite ore – Challenges in process mineralogy and impact of hydrodynamics. Miner Eng 121, 196–204. https://doi.org/10.1016/J.MINENG.2018.03.021.

Huijgen, W.J.J., Witkamp, G.J., Comans, R.N.J., 2005. Mineral CO_2 sequestration by steel slag carbonation. Environ Sci Technol 39, 9676–9682. https://doi.org/10.1021/ES050795F.

Ihinger, P.D., Zink, S.I., 2000. Determination of relative growth rates of natural quartz crystals. Nature 404, 865–869. https://doi.org/10.1038/35009091.

Iwasaki, F., Iwasaki, H., 2002. Historical review of quartz crystal growth. J Cryst Growth 237–239, 820–827. https://doi.org/10.1016/S0022-0248(01)02043-7.

Ji, G., Wang, W., Chen, H., Yang, S., Sun, J., Fu, W., Yang, B., Huang, Z., 2022. Sustainable potassium chloride production from concentrated KCl brine via a membrane-promoted crystallization process. Desalination 521, 115389. https://doi.org/10.1016/J.DESAL.2021.115389.

Ju, J., Feng, Y., Li, H., Xue, Z., Ma, R., Li, Y., 2023. Research advances, challenges and perspectives for recovering valuable metals from deep-sea ferromanganese minerals: A comprehensive review. Sep Purif Technol 315, 123626. https://doi.org/10.1016/J.SEPPUR.2023.123626.

Kilic, Ö., Kilic, A.M., 2005. Recovery of salt co-products during the salt production from brine. Desalination 186, 11–19. https://doi.org/10.1016/J.DESAL.2005.05.014.

Li, Y., Cao, B., Modali, S., Lee, E.M.Y., Xu, H., Petrenko, V., Gray, J.J., Yang, M., Mao, C., 2022. Understanding the interactions between bone mineral crystals and their binding peptides derived from filamentous phage. Mater Today Adv 15, 100263. https://doi.org/10.1016/J.MTADV.2022.100263.

Li, E., Du, Z., Yuan, S., Cheng, F., 2015. Low temperature molecular dynamic simulation of water structure at sylvite crystal surface in saturated solution. Miner Eng 83, 53–58. https://doi.org/10.1016/J.MINENG.2015.08.012.

Li, E., Duan, P., Du, Z., Li, D., Cheng, F., 2016. Colloidal properties of octadecylamine hydrochloride and the wettability of KCl crystal surface in different saturated salt solutions. J Mol Liq 223, 107–111. https://doi.org/10.1016/J.MOLLIQ.2016.08.039.

Li, X., He, F., Behrendt, F., Gao, Z., Shi, J., Li, C., 2021. Inhibition of K_2SO_4 on evaporation of KCl in combustion of herbaceous biomass. Fuel 289, 119754. https://doi.org/10.1016/J.FUEL.2020.119754.

Lin, S., Wang, C., Liu, R., Sun, W., Jing, G., 2022. Surface characterization of molybdenite, bismuthinite, and pyrite to identify the influence of pH on the mineral floatability. Appl Surf Sci 577, 151756. https://doi.org/10.1016/J.APSUSC.2021.151756.

Marion, C., Li, R., Waters, K.E., 2020. A review of reagents applied to rare-earth mineral flotation. Adv Colloid Interface Sci 279, 102142. https://doi.org/10.1016/J.CIS.2020.102142.

Monte, M.B.M., Oliveira, J.F., 2004. Flotation of sylvite with dodecylamine and the effect of added long chain alcohols. Miner Eng 17, 425–430. https://doi.org/10.1016/J.MINENG.2003.11.005.

Morse, J.W., Arvidson, R.S., Lüttge, A., 2007. Calcium carbonate formation and dissolution. Chem Rev 107, 342–381. https://doi.org/10.1021/CR050358J.

Nawaz, K., Khan, U., Ul-Haq, N., May, P., O'Neill, A., Coleman, J.N., 2012. Observation of mechanical percolation in functionalized graphene oxide/elastomer composites. Carbon N Y 50, 4489–4494. https://doi.org/10.1016/J.CARBON.2012.05.029.

Osipova, E., Shevchuk, V., Stromski, A., Romanovski, V., 2022. Intensification of potash ore flotation by the introduction of industrial oils. J. Chem. Technol. Biotechnol. 97, 312–318. https://doi.org/10.1002/JCTB.6945.

Peleka, E.N., Gallios, G.P., Matis, K.A., 2018. A perspective on flotation: a review. J. Chem. Technol. Biotechnol. 93, 615–623. https://doi.org/10.1002/JCTB.5486.

Peng, Y., Grano, S., 2010. Effect of grinding media on the activation of pyrite flotation. Miner Eng 23, 600–605. https://doi.org/10.1016/J.MINENG.2010.02.003.

Potter, R.M., Rossman, G.R., 1977. Desert Varnish: The Importance of Clay Minerals. Science 1979 (196), 1446–1448. https://doi.org/10.1126/SCIENCE.196.4297.1446.

Silva, L.F.O., Oliveira, M.L.S., Crissien, T.J., Santosh, M., Bolivar, J., Shao, L., Dotto, G.L., Gasparotto, J., Schindler, M., 2022. A review on the environmental impact of phosphogypsum and potential health impacts through the release of nanoparticles. Chemosphere 286, 131513. https://doi.org/10.1016/J.CHEMOSPHERE.2021.131513.

Tang, M., Tong, X., 2020. The relationship between anion distribution in process water and flotation properties of iron oxides. Miner Eng 154, 106378. https://doi.org/10.1016/J.MINENG.2020.106378.

Thy, P., Jenkins, B.M., Grundvig, S., Shiraki, R., Lesher, C.E., 2006. High temperature elemental losses and mineralogical changes in common biomass ashes. Fuel 85, 783–795. https://doi.org/10.1016/J.FUEL.2005.08.020.

Weedon, D., Grano, S., Akroyd, T., Goncalves, K., Moura, R., 2007. Effects of high Mg2+ concentration on KCl flotation: Part I - Laboratory research. Miner Eng 20, 675–683. https://doi.org/10.1016/J.MINENG.2007.01.006.

Wu, Z., Wang, X., Liu, H., Zhang, H., Miller, J.D., 2016. Some physicochemical aspects of water-soluble mineral flotation. Adv Colloid Interface Sci 235, 190–200. https://doi.org/10.1016/J.CIS.2016.06.005.

Xie, L., Wang, J., Lu, Q., Hu, W., Yang, D., Qiao, C., Peng, X., Peng, Q., Wang, T., Sun, W., Liu, Q., Zhang, H., Zeng, H., 2021. Surface interaction mechanisms in mineral flotation: Fundamentals, measurements, and perspectives. Adv Colloid Interface Sci 295, 102491. https://doi.org/10.1016/J.CIS.2021.102491.

Xu, L., Tian, J., Wu, H., Fang, S., Lu, Z., Ma, C., Sun, W., Hu, Y., 2018. Anisotropic surface chemistry properties and adsorption behavior of silicate mineral crystals. Adv Colloid Interface Sci 256, 340–351. https://doi.org/10.1016/J.CIS.2018.02.004.

Zhan, W., Yi, H., Song, S., Zhao, Y., Rao, F., 2019. Hydrophobic agglomeration behaviors of clay minerals as affected by siloxane structure. Colloids Surf A Physicochem Eng Asp 568, 36–42. https://doi.org/10.1016/J.COLSURFA.2019.01.061.

Zhan, W., Yuan, Y., Liu, C., Chen, P., Liang, Y., Wang, Y., Arauz-Lara, J.L., Jia, F., 2022. Preparation and application of 0D, 2D and 3D molybdenite: a review. Minerals and Mineral Materials 1, 5. https://doi.org/10.20517/mmm.2022.04.

Zhang, X., Qin, Y., Han, Y., Li, Y., Gao, P., Li, G., Wang, S., 2021. A potential ceramic ball grinding medium for optimizing flotation separation of chalcopyrite and pyrite. Powder Technol 392, 167–178. https://doi.org/10.1016/J.POWTEC.2021.07.006.

Zhang, W., Ralston, J., Sun, W., Feng, Z., Cao, J., Xu, S., Jin, X., Chen, J., Zheng, R., Gao, Z., 2023. Quantitative evaluation of collector flotation performance I: The creation of a flotation index based on mineral recovery. Sep Purif Technol 327, 124919. https://doi.org/10.1016/J.SEPPUR.2023.124919.

Zhang, Q., Sánchez-Fuentes, D., Gómez, A., Desgarceaux, R., Charlot, B., Gàzquez, J., Carretero-Genevrier, A., Gich, M., 2019. Tailoring the crystal growth of quartz on silicon for patterning epitaxial piezoelectric films. Nanoscale Adv 1, 3741–3752. https://doi.org/10.1039/C9NA00388F.

Zhou, H., Yang, Z., Zhang, Y., Han, H., He, K., Luo, X., 2021. Enhanced flotation of hemimorphite: Adjusting mineral surface potential with sodium thiocyanate as activator. Miner Eng 171, 107088. https://doi.org/10.1016/J.MINENG.2021.107088.